

# Notes

## Beaded Electrospun Fibers for Photonic Applications

Nikodem Tomczak,<sup>†</sup> Niek F. van Hulst,<sup>\*,‡</sup> and G. Julius Vancso<sup>\*,†</sup>

Materials Science and Technology of Polymers and Applied Optics group, Faculty of Science and Technology, MESA<sup>+</sup> Institute for Nanotechnology, University of Twente, P.O. Box 217, 7500 AE Enschede, The Netherlands

Received May 23, 2005

Revised Manuscript Received June 26, 2005

### Introduction

Electrospinning of polymer solutions and melts is a versatile technique used to fabricate polymer fibers with diameters ranging from  $\sim 10$  nm to several micrometers.<sup>1–6</sup> Electrospinning of various amorphous and semicrystalline polymers,<sup>7</sup> polymer blends,<sup>8</sup> and block copolymers<sup>9</sup> has been reported. Recent advances in electrospinning allowed one to perform controlled copinning of coaxial nanofibers made of two different materials.<sup>10</sup> Because of combination of low-cost instrumentation and inherent high surface-to-volume ratio of the structures obtained, electrospun fibers are finding applications in drug delivery,<sup>11</sup> membranes,<sup>12</sup> electronics,<sup>13</sup> chemical sensors,<sup>14</sup> photovoltaics,<sup>15</sup> composite materials,<sup>16</sup> and medicine.<sup>17</sup>

Recently, there is increasing interest in using polymer nanofibers in advanced photonic applications.<sup>18</sup> In this context, we,<sup>19</sup> and others,<sup>20</sup> have demonstrated the feasibility of the electrospinning technique to prepare hybrid light emitter/polymer nanofiber composites. Both organic chromophores, as well as semiconductor nanoparticles (quantum dots, QD), can be used as internal light sources. The robustness of the electrospinning technique allowed us to vary independently the polymer, the fiber diameter, and the type of the embedded light emitters.

Interestingly, apart from fibers with a broad range of diameters and made of different polymeric materials, the electrospinning method allows one also, for specific experimental conditions, to obtain other polymer structures like the “beads on a string” morphology.<sup>21–23</sup> Such morphology is a result of competing solution viscosity, capillary forces (surface tension), inertial forces, and electrostatic interactions related to the charges carried by the jet.<sup>21</sup> Size, shape, and distance between the beads can be controlled by polymer concentration, solvent used, and applied voltage. Therefore, an additional level

of structural complexity can be introduced into the fibers by the choice of suitable spinning conditions.

The micrometer size and spherical shape of the polymer beads suggest that these structures will have interesting photonic properties, similar to those found in dielectric microspheres<sup>24</sup> or suspended micrometer liquid droplets.<sup>25</sup> It is therefore important to investigate in more detail the structure and photonic properties of beaded polymer fibers and properties of the beads in particular.

In this contribution we describe results obtained by investigating the structure and photonic properties of polymer beads by fluorescence microscopy down to the single molecule level. We investigated beads formed from poly(methyl methacrylate) and poly(ethylene oxide) and found that the chromophores are differently distributed over the bead volume, indicating different internal structures of the beads. The effect of the fiber and bead confinement on the emission properties of embedded dyes was studied by monitoring their fluorescence lifetime. The fluorescence lifetime of the embedded dyes was found to depend on the material used. As a reason for such a behavior, possible quenching and electromagnetic boundary effects are discussed.

### Experimental Section

The electrospinning device consisted of a capillary (tip diameter 2 mm), which included a wire electrode, a grounded counter electrode placed 12 cm from the capillary, and a high-voltage source. The flow rate of the polymer solution was equal to 100  $\mu\text{L}/\text{min}$ . The potential between the electrodes was adjusted with a high-voltage power supply (Bertan Series 230). More details about the electrospinning method and the electrospinning device used in this study can be found elsewhere.<sup>5,16</sup> As a substrate, circularly shaped glass cover slides (diameter = 20 mm, Fisher Scientific) were employed. Prior to electrospinning, the slides were cleaned using a Piranha solution (mixture of 1:4 of 30%  $\text{H}_2\text{O}_2$  and concentrated  $\text{H}_2\text{SO}_4$ ), rinsed with Milli-Q water and ethanol, and finally dried in a stream of nitrogen gas. Samples of luminescent polymer fibers were prepared by electrospinning polymer solutions containing 1,1',3,3',3',3'-hexamethylindodicarbocyanine ( $\text{DiIC}_1(5)$ ) molecules ( $10^{-9}$  M, Molecular Probes, D-307) directly onto the glass cover slides. The diameter and morphology of the fibers were tuned by the concentration of the polymer in the spun solutions, the applied voltage between the electrodes, and the distance between the electrodes. A solution of 12.5 wt % of poly(methyl methacrylate) (PMMA,  $M_w = 120$  kg/mol, Aldrich) in acetone was spun under a potential of 12 kV. Poly(ethylene oxide) (PEO,  $M_w = 2000$  kg/mol, Aldrich) fibers were obtained using a 0.5 wt % chloroform solution and by spinning at 8 kV.

**Scanning Confocal Microscopy.** For excitation and time-resolved experiments a picosecond-pulsed dye laser (635 nm, PicoQuant, 800-B, 100 mW, 80 MHz repetition rate) was used. The excitation light was made circularly polarized by a  $1/4\lambda$  plate and focused onto the sample to a diffraction-limited spot using a high NA oil objective (Olympus, NA = 1.4, 100 $\times$ ). To separate the fluorescence emission from the excitation, suitable dichroic mirrors, emission, and excitation filters were used. Fluorescence photons were collected by the same objective and

<sup>†</sup> Materials Science and Technology of Polymers.

<sup>‡</sup> Applied Optics group.

\* Corresponding authors. N.F.v.H.: tel +31534893172, fax +31534893511, e-mail n.f.vanhulst@tnw.utwente.nl. G.J.V.: tel +31534892967, fax +31534893823, e-mail g.j.vancso@tnw.utwente.nl.

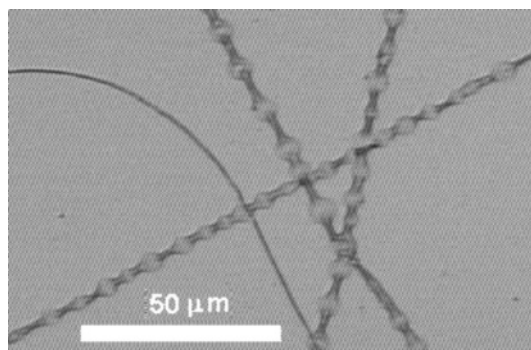


**Figure 1.** Optical micrograph of electrospun poly(ethylene oxide) fibers exhibiting a “beads on a string” morphology.

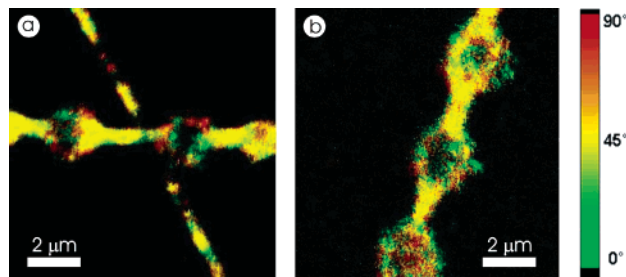


**Figure 2.**  $10 \times 10 \mu\text{m}^2$  fluorescence intensity scans of beaded PEO fibers. The color scale indicates the orientation of the emission dipole moment of the molecules. Diffraction limited, constant-polarization spots visible at the bead edges indicate single molecule emission. The DiIC<sub>1</sub>(5) molecules in PEO beads are mostly located near the bead edges.

sent to two avalanche photodetectors (SPCM-AQ-14, EG&G Electro Optics) placed after a polarization beam splitter. The sample was scanned through the focus of the excitation spot at a pixel frequency of 1 kHz, producing two-dimensional ( $256 \times 256$  pixels) fluorescence intensity images (including two independent polarization channels). For time-resolved experiments the detected fluorescence signal was fed into a time-correlated single photon counting card (TCSPC, SPC 500).<sup>26</sup>

**Wide-Field Microscopy.** Light from a He–Ne laser at a wavelength of 632 nm was used for excitation. A circularly polarized laser beam passed through a beam expander and was focused onto the back aperture of a high NA objective (Zeiss, NA = 1.4). The fluorescence was collected by the same objective and after passing through emission filters was split into two polarization channels using a Wollaston prism (Linios 037808) and subsequently imaged with a 500 mm lens (Linios 063827) onto an intensified charged coupled device (CCD camera, Pentamax Gen IV). The images from the camera were processed by custom LabView software.

**Bright Field Imaging.** Bright field images were obtained using an Olympus BX 60 light microscope or by placing an intense light source above the samples and collecting the transmitted light using a CCD camera placed on one of the ports of the confocal microscope or using the CCD camera in the wide-field setup.

## Results and Discussion

In Figure 1 fibers with almost evenly spaced PEO beads are shown. A broad distribution of the diameter values of the beads (ranging from several hundreds of nanometers to several micrometers) could be observed. The use of high resolution and sensitivity fluorescence microscopy allows us to perform single molecule photophysical investigations of the influence of the fiber shape and size on the fluorescence emission characteristics of the light emitters.<sup>19</sup> Figure 2 shows  $10 \times 10 \mu\text{m}^2$  fluorescence intensity scans of DiIC<sub>1</sub>(5) molecules embedded in beads formed along PEO fibers. Fluores-

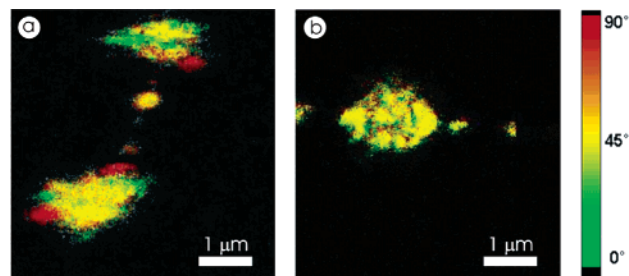


**Figure 3.**  $5 \times 5 \mu\text{m}^2$  fluorescence intensity scans of beaded PMMA fibers. In the case of PMMA fibers the chromophores are distributed over the entire bead volume. Also, molecules along the fibers connecting the beads are visible.

cence emission spectra collected from individual fibers and beads confirmed that the fluorescence is indeed coming from DiIC<sub>1</sub>(5) molecules (not shown here).<sup>19</sup> The color scale is an indication of the in-plane polarization of the fluorescence. In some parts of the fibers diffraction limited fluorescence spots with a specific polarization direction are visible, indicating single molecule emission from within the fibers. It should be noted that both single dyes with orientation in between the axis of the two orthogonal detectors and a collection of dyes with random orientation will appear “yellow” on the pictures.

Remarkably, the scanning confocal images show that the dyes are not uniformly distributed within the PEO beads but are concentrated around the bead edges. When embedding DiIC<sub>1</sub>(5) in beads made of PMMA (Figure 3), the dyes were not located at the bead edges anymore but were distributed over the entire bead volume. This surprising effect the choice of the polymer has on the distribution of dyes within the beads motivated us to perform additional experiments. We imaged the fibers using a wide field fluorescence microscope (WFM). WFM allows one to check whether the patterns observed are due to distortions of the excitation focus by the beads. Parts a and b of Figure 4 show the fluorescence emitted by DiIC<sub>1</sub>(5) molecules embedded in PMMA and PEO fibers, respectively. Clearly, the PMMA beads are filled with molecules over the entire bead volume; however, the chromophores are absent from the PEO bead interior. The differences found for PMMA and PEO can be explained by the possibility that the dyes are being excluded from the semicrystalline phase of PEO during the crystallization process, which takes place in the central regions of the beads. In contrast, PMMA being amorphous allows the dyes to be distributed within the entire volume of the bead. An intriguing feature in the images of PEO beads is a small fluorescence spot almost exactly in middle of each bead (Figure 4b–d). This is likely due to the focusing effect of such large, micrometer size, dielectric beads, as described earlier in the literature e.g. by Barnes et al.<sup>25</sup> Beads made of PMMA should also display such focusing effects; however, because of the presence of molecules distributed all over the PMMA bead, such emission spots are overshadowed by the overall emission intensity and could not be clearly identified. Indeed, when applying high laser excitation power and bleaching the majority of the chromophores in the bead, the center spots could be visualized. Wide-field experiments revealed additionally that the dye molecules might have an induced orientation inside the beads. Figure 4d shows a polarization-resolved picture of DiIC<sub>1</sub>(5) molecules in a PEO bead. Even though the beads contained large amounts of chromophores, remarkably, our results

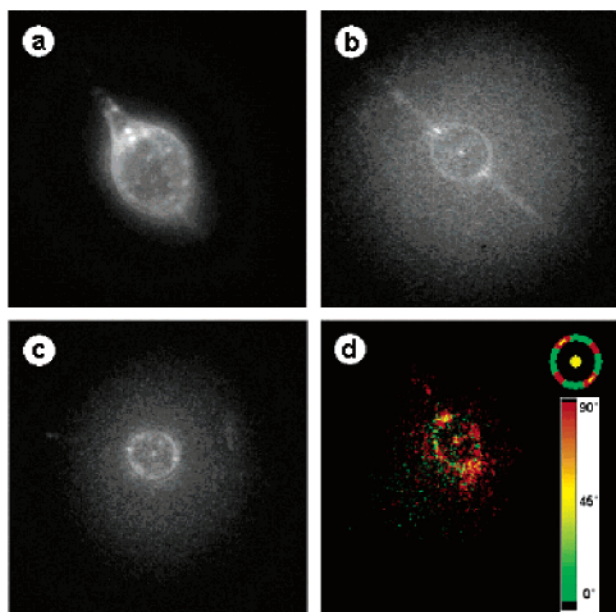


**Figure 4.** Fluorescence images of DiIC<sub>1</sub>(5) molecules in polymer beads imaged with a wide-field microscope. An area of 380  $\mu\text{m}^2$  (22  $\mu\text{m}$  in diameter) is being illuminated. Parts (a) and (b) show fluorescence from DiIC<sub>1</sub>(5) molecules embedded in PMMA and PEO beads, respectively. In contrast to PMMA, there is no significant fluorescence signal coming from within the PEO beads (b, c). Additionally, a peculiar, almost diffraction limited spot is clearly visible in the center of each PEO bead (b–d). For PEO beads, the fluorescence has a well-defined polarization even though a large amount of DiIC<sub>1</sub>(5) molecules is embedded within the structure (d). The color scale indicates the fluorescence polarization in two orthogonal channels. The inset in (d) shows an extracted polarization pattern.

indicate that the emission from different parts of the bead is strongly polarized. This indicates that the chromophores adopt a preferred orientation at the bead edges. The inset of Figure 4d shows the scheme of the extracted polarization pattern. The pattern suggests a complex relationship between fiber direction and chromophore molecular orientation in the beads. Bead size, processing history, and internal structure can influence molecular orientation. More careful investigations of the distribution of orientations of the embedded chromophores, especially at the single molecule level, could help to solve some questions related to internal molecular level structure of the electrospun fibers.

Finally, using the scanning confocal microscope equipped with a TCSPC card, we have measured fluorescence lifetimes of DiIC<sub>1</sub>(5) molecules at different positions in individual PEO and PMMA fibers, and beads, and compared these to the fluorescence lifetime found for DiIC<sub>1</sub>(5) embedded in thick polymer films. While the fluorescence lifetime of DiIC<sub>1</sub>(5) in the straight parts of PEO fibers was essentially the same as in thick PEO samples ( $\sim 2.3$  ns), the fluorescence lifetime of molecules embedded at the bead edges was shorter by almost 25% ( $\sim 1.7$  ns). Remarkably, the fluorescence lifetime of DiIC<sub>1</sub>(5) molecules in PMMA beads displayed the opposite behavior. The fluorescence lifetime of DiIC<sub>1</sub>(5) at the bead center and in the straight fiber parts was equal to the bulk value ( $\sim 2.2$  ns). At the edges of the beads, however, DiIC<sub>1</sub>(5) molecules were decaying from their excited state almost twice as slow, and the excited-state lifetime approached an average of 4.2 ns. The similar value of the dielectric constant of PEO and PMMA indicates that such obser-

vations are not solely due to the material used, but other factors should also play a role. One of the possible explanations of this intriguing result is the interplay between quenching and electromagnetic boundary effects. For PEO beads DiIC<sub>1</sub>(5) molecules can be located at the bead surface (on top of the polymer crystals) and be exposed to the surrounding air. In the case of PMMA the molecules are embedded in the polymer, and quenching is prevented. For PMMA the electromagnetic boundary conditions would become dominant, especially for chromophores located close to the polymer/air interface, with a perpendicular orientation of the emission dipole moment.<sup>26</sup> In the case of PEO the chromophores at the surface sites are more sensitive to quenching, and therefore the fluorescence lifetime is on average lower. However, to answer the question of whether the reported behavior of the fluorescence lifetime is due to the location and organization of the chromophores in the beads, a more detailed investigation is required, preferably at the single molecule level.

## Conclusions

Luminescent PEO and PMMA fibers with “beads on a string” morphology were prepared by electrospinning. Depending on the material used to spin, polymer beads with different spatial distributions of the embedded chromophores were obtained. The chromophores in PMMA beads were evenly distributed over the bead volume. In contrast to PMMA, the chromophores in PEO beads were located mainly at the bead edges, probably due to the exclusion from the PEO crystalline phase. Additionally, polarization-resolved experiments showed that the chromophores in PEO beads have a well-defined orientation. Time-resolved experiments showed that the excited-state lifetime of the dyes embedded at the bead edges was different than in straight parts of the fibers or in polymer films and displayed an opposite behavior for PMMA and PEO. Such differences were attributed to the interplay between quenching and electromagnetic boundary effects.

**Acknowledgment.** We thank Lanti Yang and Shuying Gu for their experimental work with the electrospinning setup. The Council for Chemical Sciences of the Netherlands Organization for Scientific Research (NWO-CW) is acknowledged for financial support of this research (N.T.).

## References and Notes

- (1) Formhals, A. U.S. Patent 2,116,942, 1938.
- (2) Srinivasan, G.; Reneker, D. H. *Polym. Int.* **1995**, *36*, 195.
- (3) Doshi, J.; Reneker, D. H. *J. Electrostat.* **1995**, *35*, 151.
- (4) Reneker, D. H.; Chun, I. *Nanotechnology* **1996**, *7*, 216.
- (5) Jaeger, R.; Bergshoef, M. M.; Battle, C. M. I.; Schönherr, H.; Vancso, G. J. *Macromol. Symp.* **1998**, *127*, 141.
- (6) Bognitzki, M.; Czado, W.; Frese, T.; Schaper, A.; Hellwig, M.; Steinhart, M.; Greiner, A.; Wendorff, J. H. *Adv. Mater.* **2001**, *13*, 70.
- (7) Jaeger, R.; Schönherr, H.; Vancso, G. J. *Macromolecules* **1996**, *29*, 7634.
- (8) Norris, I. D.; Shaker, M. M.; Ko, F. K.; MacDiarmid, A. G. *Synth. Met.* **2000**, *114*, 109.
- (9) Fong, H.; Reneker, D. H. *J. Polym. Sci., Part B: Polym. Phys.* **1999**, *37*, 3488.
- (10) Sun, Z. C.; Zussman, E.; Yarin, A. L.; Wendorff, J. H.; Greiner, A. *Adv. Mater.* **2003**, *15*, 1929.
- (11) Kawanay, E. R.; Bowlin, G. L.; Mansfield, K.; Layman, J.; Simpson, D. G.; Sanders, E. H.; Wnek, G. E. *J. Controlled Release* **2002**, *81*, 57.
- (12) Gibson, P.; Schreuder-Gibson, H.; Rivin, D. *Colloids Surf., A* **2001**, *187*, 469.

- (13) Pinto, N. J.; Johnson, A. T.; MacDiarmid, A. G.; Mueller, C. H.; Theofylaktos, N.; Robinson, D. C.; Miranda, F. A. *Appl. Phys. Lett.* **2003**, *83*, 4244.
- (14) Wang, X. Y.; Drew, C.; Lee, S. H.; Senecal, K. J.; Kumar, J.; Samuelson, L. A. *J. Macromol. Sci.* **2002**, *A39*, 1251.
- (15) Drew, C.; Wang, X. Y.; Senecal, K.; Schreuder-Gibson, H.; He, J. N.; Kumar, J.; Samuelson, L. *J. Macromol. Sci., Part A* **2002**, *A39*, 1085.
- (16) Bergshoef, M. M.; Vancso, G. J. *Adv. Mater.* **1999**, *11*, 1362.
- (17) Li, W. J.; Laurencin, C. T.; Catterson, E. J.; Tuan, R. S.; Ko, F. K. *J. Biomed. Mater. Res.* **2002**, *60*, 613.
- (18) Dersch, R.; Steinhart, M.; Boudriot, U.; Greiner, A.; Wendorff, J. H. *Polym. Adv. Technol.* **2005**, *16*, 276.
- (19) Tomczak, N.; Gu, S.; Han, M.; van Hulst, N. F.; Vancso, G. J., submitted for publication.
- (20) Schlecht, S.; Tan, S.; Yosef, M.; Dersch, R.; Wendorff, J. H.; Jia, Z.; Schaper, A. *Chem. Mater.* **2005**, *17*, 809.
- (21) Lee, K. H.; Kim, H. Y.; Bang, H. J.; Jung, Y. H.; Lee, S. G. *Polymer* **2003**, *44*, 4029.
- (22) Fong, H.; Chun, I.; Reneker, D. H. *Polymer* **1999**, *40*, 4585.
- (23) Hsu, C.; Shivkumar, S. *J. Mater. Sci.* **2004**, *39*, 3003.
- (24) Schiro, P. G.; Kwok, A. S. *Opt. Express* **2004**, *12*, 2857.
- (25) Barnes, M. D.; Kung, C.-Y.; Whitten, W. B.; Ramsey, J. M.; Arnold, S.; Holler, S. *Phys. Rev. Lett.* **1996**, *76*, 3931.
- (26) Vallée, R. A. L.; Tomczak, N.; Gersen, H.; van Dijk, E. M. H. P.; García-Parajó, M. F.; Vancso, G. J.; van Hulst, N. F. *Chem. Phys. Lett.* **2001**, *348*, 161.

MA051049Y